Validity of the scattering-length approximation in strongly interacting Fermi systems

S. Q. Zhou, D. M. Ceperley, and Shiwei Zhang

Phys. Rev. A **84**, 013625 — Published 29 July 2011

DOI: 10.1103/PhysRevA.84.013625

Validity of the scattering length approximation in strongly interacting Fermi systems

S. Q. Zhou and D. M. Ceperley
Department of Physics and NCSA, University of Illinois at Urbana-Champaign, Urbana, Illinois 61801, USA

Shiwei Zhang
Department of Physics, College of William and Mary, Williamsburg, Virginia 23187, USA

We investigate the energy spectrum of systems of two, three and four spin-$\frac{1}{2}$ fermions with short range attractive interactions both exactly, and within the scattering length approximation. The formation of molecular bound states and the ferromagnetic transition of the excited scattering state are examined systematically as a function of the 2-body scattering length. Identification of the upper branch (scattering states) is discussed and a general approach valid for systems with many particles is given. We show that an adiabatic ferromagnetic transition occurs, but at a critical transition point $k_F a$ much higher than predicted from previous calculations, almost all of which use the scattering length approximation. In the 4-particle system the discrepancy is a factor of 2. The exact critical interaction strength calculated in the 4-particle system is consistent with that reported by experiment. To make comparisons with the adiabatic transition, we study the quench dynamics of the pairing instability using the eigenstate wavefunctions.

PACS numbers: Valid PACS appear here

I. INTRODUCTION

The control afforded by Feshbach resonance phenomena in ultracold atomic gases has enabled the exploration of strongly correlated degenerate Fermi systems. In a recent study of the possibility of itinerant ferromagnetism [1–4], Jo *et al.* [5] attempted to observe the physics behind the Stoner model in an atomic gas of ^{6}Li atoms. Evidence for ferromagnetic ordering was seen. This experiment has generated a great deal of theoretical research [6–11]. The results have been debated as to whether a ferromagnetic transition or a strong correlation effect was seen. Quantitative comparison with experiment has not been achieved.

A key issue is to find an appropriate model for the experiment. In the experiment a strong attractive interaction is quickly switched on. Predictions of the critical ratio of interaction strength to interatomic spacing for the ferromagnetic transition from mean field theory [3, 6], second order corrections [4, 7] and QMC calculations [8–10] are on the order of $k_F a \sim 1$; about two times lower than that from the Jo *et al.* experiment. In almost all calculations, a positive interaction [8, 9] or a Jastrow factor with two-body nodes [10] is assumed, using the scattering length approximation(SLA). Moreover, the various approaches differ in details of the nature of the transition [3, 4].

The two-body SLA neglects the low-lying molecular states. The zero-energy s-wave scattering length a is defined by the long distance form of the out-going scattering wave

$$\psi\left(r \to \infty\right) \propto \frac{\sin\left[k(r-a)\right]}{kr} \overset{k\to 0}{\longrightarrow} 1 - \frac{a}{r}. \qquad (1)$$

For a contact (zero range) potential, a is the radius of the first wavefunction node: $\psi\left(r=a\right)=0$. The SLA replaces the underlying atomic interaction by a purely repulsive potential which has the same two-body scattering length.

This is analogous to the idea of pseudo-potentials in electronic structure. A pseudo-potential can be generated in an atomic calculation to replace the strong Coulomb potential of the nucleus and the effects of the tightly bound core electrons by an effective ionic potential acting on the valence electrons and then used to compute properties of valence electrons in molecules or solids, since the core states remain almost unchanged. The approach is widely used in electronic structure calculations. However, it leads to an inaccuate model if a pseudopotential is used for systems compressed to high density and the electron cores start to overlap.

Many experiments in cold atomic systems are performed near Feshbach resonance where the scattering length is comparable to interatomic separation. In this situation, the lower-lying molecular bound states giving rise to resonance can overlap, causing the scattering states to distort in order to remain orthogonal to the bound states. With more experimental effort expected in the study of related systems, precise and reliable comparisons from quantum simulations will be important. Yet accurate many-body calculations will not be possible without a quantitative understanding of the effective interactions and their effect on the different states. Even the identification of the scattering state in a dense system requires explanation.

In this article, we quantify this effect by explicitly including the molecular bound states and treating the interaction exactly. We consider systems of two, three and four spin-$\frac{1}{2}$ fermions interacting through a contact interaction. The energy spectrum as a function of the two-body interaction strength is obtained by using an exact numerical method on a lattice and then extrapolated to the continuum limit. We show how the upper branch can be identified for a many-body system. The properties of

the nodal surface of the scattering many-body states are investigated. To compare with the exact solutions, calculations are also made with the SLA, by replacing the attractive contact interaction with a zero boundary condition. In both cases an adiabatic ferromagnetic transition is stabilized. The SLA breaks down for large a, leading to a severe underestimation (by almost a factor of 2) of the transition point.

II. METHOD

We consider a system of two-component fermions moving in a periodic box with length L to model a gas of ^{6}Li atoms with two hyperfine species at non-zero density. All lengths are expressed in units of L and all energies in units of $K_0 = \frac{\hbar^2}{2m}(\frac{2\pi}{L})^2$. In the case $a \gg r_0$ (where r_0 is a measure of the effective interaction range), the interatomic potential can be modeled as a regularized δ-function:

$$V(\mathbf{r},\mathbf{r}') = \frac{4\pi\hbar^2 a}{m}\delta(\mathbf{r}-\mathbf{r}')\frac{\partial}{\partial|\mathbf{r}-\mathbf{r}'|}|\mathbf{r}-\mathbf{r}'| \qquad (2)$$

where a is the zero-energy scattering length and m is the mass. We solve the Schrödinger equation by putting the system on a lattice with n points in each direction and recover the continuum limit by extrapolation. We then approximate the kinetic energy by two different discrete Laplacian operators [13]: (1) the Hubbard model with nearest neighbor hopping and (2) a long range hopping model including up to the next nearest neighbors. We model the bare two-particle interaction by a point contact potential on the grid

$$V^{\rm grid}(\mathbf{r},\mathbf{r}') = -\frac{U}{\Delta^3}\delta_{\mathbf{r},\mathbf{r}'}, \qquad (3)$$

where $\Delta = L/n$ is the grid spacing. Here $U > 0$ is the strength of the attractive interaction; on the repulsive side of resonance $U > U_\infty$, we have positive scattering length for unpaired atoms and the mapping relation between the grid and continuum is [15]

$$\frac{m}{4\pi\hbar^2 a} = \frac{1}{U_\infty} - \frac{1}{U}, \qquad (4)$$

where the unitarity point $a \to \infty$ occurs at $U_\infty^{-1} = (2\pi)^{-3}\int d^3\mathbf{k}(2\epsilon_\mathbf{k})^{-1} = \gamma m/(\hbar^2\Delta)$. Here $\epsilon_\mathbf{k}$ is the single particle dispersion relation and γ is a numerical constant defined by the discrete Laplacian. For choice (1) above, $\gamma \approx 0.2527$; for choice (2), $\gamma \approx 0.2190$. When only nearest neighbor hopping is included, our Hamiltonian is the standard attractive Hubbard model, but scaled by $1/\Delta^2$. Note our U value scales as Δ, while in the notation of the Hubbard model, U_∞ is a constant.

In the SLA, U has the opposite sign. In particular, when the scattering length a is large, Eq. (3) is replaced by a hard-sphere potential with radius a. If a is smaller than the grid spacing, a finite but negative value of U can be used in the SLA, leading to the repulsive Hubbard model, which clearly has a different strongly interacting or large a limit [11] from that of Eq. (3).

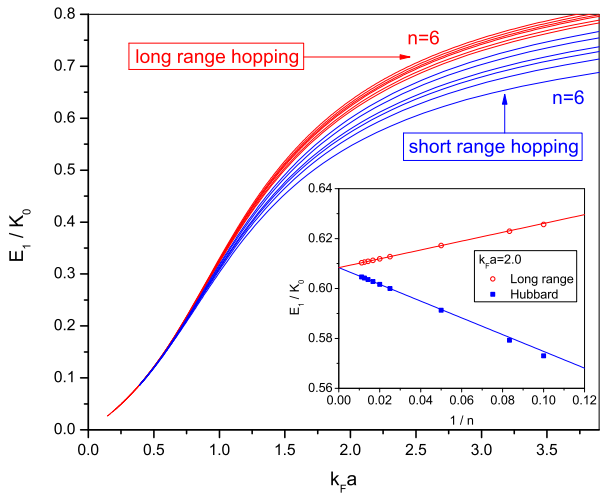

FIG. 1: (Color online) The two-body s-wave scattering energy E_1 as a function of $k_F a$ for grid sizes: $n = 6, 8, 10, 12, 20, 40$. The inset shows the scaling with respect to $1/n$ at $k_F a = 2.0$ with grid sizes up to $n = 90$. The long-range hopping model converges to the continuum limit faster than the Hubbard model.

To determine the eigenvalues and eigenstates, we start from a set of random trial states $|\psi_\alpha^0\rangle$ where $1 \le \alpha \le M$, and evolve the states $|\psi^{i+1}\rangle = (\mathbf{1} - \tau\hat{H})|\psi^i\rangle$. At each step of the evolution, the state vectors are properly symmetrized and orthogonalized. As $i \to \infty$, the states converge to the lowest M eigenstates of the Hamiltonian $\hat{H}$ within a given symmetry sector. The errors are controlled and can be reduced arbitrarily with increasing the number of grid points or number of iterations. As discussed below, the computational cost grows rapidly with system size, but significant reduction can be achieved by invoking symmetries.

To assess the accuracy of iterative diagonalization, we test the method on a two-particle problem. The energy of the lowest two-particle scattering state is plotted in Fig (1) as a function of the dimensionless scattering length $k_F a$, where $k_F = (3\pi^2\rho)^{1/3}$ is the Fermi wave vector and ρ the particle density. Both discrete representations of the kinetic energy operator were used and they converge to the same continuum limit: $n \to \infty$; the long-range hopping is found to be less sensitive to the lattice spacing. Solving the two-particle problem also enables us to construct repulsive pseudo-potentials in the SLA by inverting the 2-particle Schrödinger equation.

III. TWO FIXED POINT POTENTIALS

The simplest case where the scattering length approximation may fail is the scattering of a single particle off of

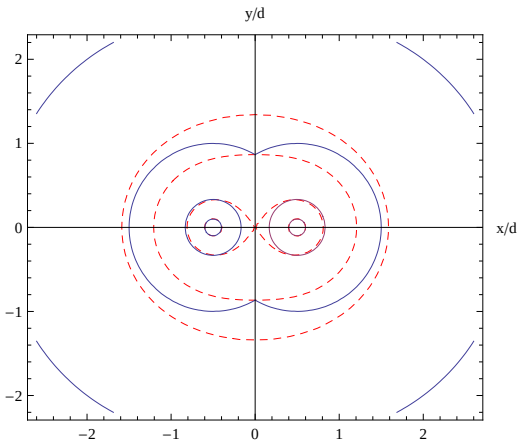

FIG. 2: (Color online) Nodal surface for the scattering wavefunction in a potential generated by two fixed particles located at $(\pm d/2, 0, 0)$ in infinite space with $a/d = 1/10, 1/3, 1, 5/2$ (expanding outward), where d denotes the distance between the two fixed scatterers. The solid (blue) lines correspond to the nodes in SLA and the dashed (red) lines to the exact nodes. SLA gives a reasonable approximation to the nodal surface for $a/d < 1$ but the deviation becomes significant for large scattering lengths.

two fixed contact potentials. This problem can be solved exactly in infinite space [16]. The nodal surface of the zero-energy scattering state is given as the solution of:

$$\frac{1}{|\mathbf{r}-\mathbf{R}_1|}+\frac{1}{|\mathbf{r}-\mathbf{R}_2|}=\frac{1}{a}+\frac{1}{|\mathbf{R}_1-\mathbf{R}_2|}, \qquad (5)$$

where $\mathbf{R}_1$ and $\mathbf{R}_2$ are the location of the two fixed scatterers. In the SLA, one would model the state by the ground state with nodes defined by $|\mathbf{r}-\mathbf{R}_1| = a$ and $|\mathbf{r}-\mathbf{R}_2| = a$. The nodal surfaces described by Eq. (5) are shown in Fig (2) in comparison with corresponding spheres in SLA. Clearly the deviation from SLA becomes significant as $a \sim |\mathbf{R}_1 - \mathbf{R}_2|$. In particular, the spherical surfaces in SLA becomes infinitely large at unitarity limit while Eq. (5) gives rise to a finite surface. This result suggests that introducing a node in the two-body Jastrow factor in the form $f(r) \sim (1 - a/r)$ is insuffcient to characterize the effective pairwise repulsion on the upper-branch [10], as further discussed below in Sec.VI.

To study the effect of the SLA at finite density, we solved the same problem numerically in a finite periodic box. The results are summarized in Fig (3). It can be seen from the graph that at large scattering length (i.e. at high density), the SLA significantly overestimates the scattering energy for the 3-body problem, i.e. the effect of low-lying molecular states cannot be ignored. The exact solution achieves a lower energy by distorting the nodal surfaces away from the union of two spheres required by the SLA. As we show below, this also applies to a system of more fermions.

IV. FOUR-PARTICLE MODEL

Now consider a minimal model for the ferromagnetic transition: four spin-$\frac{1}{2}$ atoms in a cube with periodic boundary conditions and interacting with a contact potential. The spin polarized state $\Psi(1234) = \psi_A(1234) \otimes |\uparrow\uparrow\uparrow\uparrow\rangle$ has a totally antisymmetric spatial part $\psi_A(1234)$: for a contact interaction it is noninteracting with an energy of $4K_0$ in a zero total momentum eigenstate that has translational invariance. On the other hand, there are two linearly independent spin states with zero total spin $S^2 = 0$ corresponding to unpolarized states:

$$\chi_{MS} \propto |\uparrow\uparrow\downarrow\downarrow\rangle + |\downarrow\downarrow\uparrow\uparrow\rangle - \frac{1}{2}\big[\,|\uparrow\downarrow\rangle + |\downarrow\uparrow\rangle\,\big] \otimes \big[\,|\uparrow\downarrow\rangle + |\downarrow\uparrow\rangle\,\big],$$
$$\chi_{MA} \propto \big[\,|\uparrow\downarrow\rangle - |\downarrow\uparrow\rangle\,\big] \otimes \big[\,|\uparrow\downarrow\rangle - |\downarrow\uparrow\rangle\,\big].$$

The wavefunction is a linear combination of the above two states $\Psi(1234) = \psi_{MA} \otimes \chi_{MS} + \psi_{MS} \otimes \chi_{MA}$. The symmetries of ψ_{MA} and ψ_{MS} in coordinate-space are determined by the total antisymmetry of the complete wavefunction including spins and coordinates.

For a system of four particles on a grid with n points in each direction, the discretized configuration space has n^{12} grid points. Translational symmetries along the three spatial directions reduce the size of the configuration space by a factor of n^3. Cubic symmetry of the periodic box reduces the number of independent wavefunction values by a factor of 48 and permutation symmetries give an additional 24-fold reduction. We evolve pairs of non-magnetic states $\{\psi_{MS}, \psi_{MA}\}$ within the reduced domain, and whenever the value of the wavefunctions on a grid point outside the reduced domain is needed in off-diagonal projections, the exterior point is mapped back into the reduced domain by symmetry transformations.

The ferromagnetic transition is identified as the crossing between the lowest singlet scattering state and the fully ferromagnetic state. To investigate the effect of using the SLA in multi-particle scattering process, the attractive contact interaction is replaced by a zero boundary condition and the resulting critical ferromagnetic density is estimated.

Fig (4) shows the energy spectrum of a four-particle system for $n = 10$ as a function of the coupling coefficient U. In this calculation, the lowest 30 states were followed. Note that we only considered states with the same symmetries as the ground state, i.e. with even parity with respect to reflection in x, y or z. The resulting energy levels can be classified into three categories by their behavior at strong coupling: two-molecule states, molecule-atom-atom states and four-atom scattering states. Level avoiding [17] can be observed between states belonging to different categories.

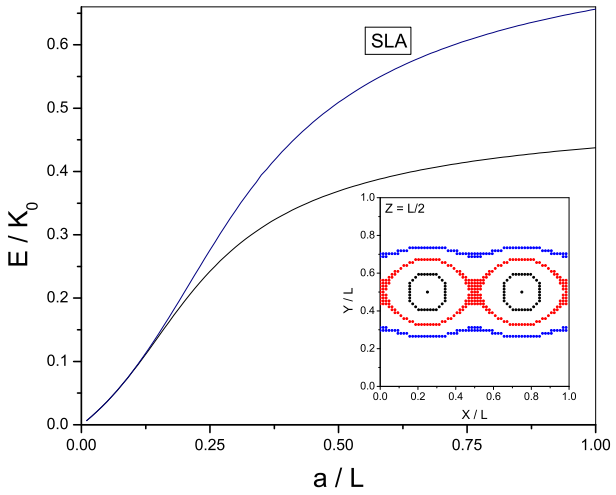

FIG. 3: (Color online) The scattering energy of a particle moving in the potential generated by two fixed particles located at $x = L/4$ and $x = 3L/4$, with $y = L/2$ and $z = L/2$. The SLA is obtained by replacing each potential by a hard sphere (zero boundary condition) with the same scattering length. The SLA gives accurate energies in weakly-interacting limit ($a/L < 0.2$) but overestimates the scattering energy for a comparable with L. The inset shows the nodal region ($|\psi_i| < 10^{-4}$) for the scattering states with $a/L = 0.1(\text{black}), 0.2(\text{red}), 0.4(\text{blue})$. The surfaces become noticeably non-spherical for $a/L > 0.1$.

V. IDENTIFICATION OF THE SCATTERING STATES

The formation of molecular bound states is characterized by the binding energy diverging linearly as $U \to \infty$. In particular, the ground state wavefunction can be approximately written as $\psi_0(13)\psi_0(24) - \psi_0(14)\psi_0(23)$ where ψ_0 is the two-body bound state, and the ground state energy is approximately twice the two-particle binding energy. As seen in Fig. (3) the two-molecule states have an energy slope $(\partial E/\partial U)$ about twice as large as the molecule-atom-atom states. As $U \to \infty$ molecules become tightly bound; their energy spacings can be understood in terms of colliding molecules. For a lattice model, in contrast to a continuum model, the greater the internal binding energy, the greater the total mass of the molecule [18].

The scattering state of strongly repulsive atoms is an excited branch and all cold atom experiments performed in this regime are metastable. In Jo *et al.* experiment, the magnetic field ramp (~ 4.5ms) is much slower compared to the characteristic time scale of atomic collisions $\hbar/k_B T_F \sim \mu$s, and marches toward the resonance from the repulsive side $a \gtrsim 0$. At low density or in the weakly interacting regime, the four-atom scattering state approaches the noninteracting line $2K_0$ and the SLA is an accurate approximation. But there are some difficulties in defining the scattering state at high density or in the strongly interacting regime because of the level avoiding phenomena. As shown in the inset of Fig (4), if the coupling coefficient U is tuned toward the resonance U_∞, it is energetically more favorable to jump through the successive avoided crossings. Thus, the change in the scattering energy due to an adiabatic tuning of the interaction can then be determined by following the excited branch curve. It is drawn in bold in Fig (4).

There is another way to identify the upper branch (scattering states) quantitatively by using the momentum distribution and the pairing order. First, consider the wavefunctions for the relative motion of two particles interacting through a large scattering length of Eq. (2). The zero-energy scattering state in coordinate space $\psi(\mathbf{r}) \propto r^{-1} - a^{-1}$ takes the form $\psi(\mathbf{k}) \propto 4\pi k^{-2} - (2\pi)^3 a^{-1}\delta(\mathbf{k})$ in momentum space and diverges at $\mathbf{k} = 0$. By contrast, the bound state $\psi(\mathbf{r}) \propto r^{-1}e^{-r/a}$ takes the form $\psi(\mathbf{k}) \propto 4\pi(k^2 + a^{-2})^{-1}$ in momentum space and remains finite at $\mathbf{k} = 0$. The momentum distribution $n(\mathbf{k})$ for scattering states is different from bound states at $\mathbf{k} = 0$: scattering states have a larger fraction of particle occupation at $\mathbf{k} = 0$.

We also consider the pairing order defined by:

$$g_2 \equiv n\Big\langle \sum_{i<j} \delta_{\mathbf{r}_i,\mathbf{r}_j} \Big\rangle_\alpha \tag{6}$$

for each state $|\psi_\alpha\rangle$. The quantity g_2 measures double occupancy, and is related to the energy slope:

$$\frac{\partial E_\alpha}{\partial U} = \Big\langle \frac{\partial \hat{H}}{\partial U} \Big\rangle_\alpha = -\frac{1}{\Delta^2 L} g_2. \tag{7}$$

For the scattering state, double occupancy decreases monotonically as the interaction strength is increased (see e.g. Ref. [11]). Thus the scattering state in each lattice system is characterized by a vanishing energy slope as $U \to \infty$,

$$g_2 \to 0, \quad \frac{\partial E_\alpha}{\partial U} \to 0, \tag{8}$$

as can be seen in Fig (4). The pairing density is also related to the tail of the momentum distribution, which describes the short range physics. At large k, the momentum distribution takes the form $n(\mathbf{k}) \to C/k^4$, where the coefficient C is called the *contact* in the Tan relations [19]. In the continuum limit $\Delta \ll a$, the contact C can be related to the energy slope, and hence g_2, through the adiabatic sweep theorem $\frac{dE}{da^{-1}} = -\frac{\hbar^2}{4\pi m} C$, which in our system yields:

$$g_2 = L\Big[\gamma - \frac{\Delta}{4\pi a}\Big]^2 C, \tag{9}$$

where γ is the numerical constant appearing in the definition of U_∞. For bound states this gives a finite g_2 and a finite energy slope.

Thus, in addition to the momentum distribution at $\mathbf{k} = 0$, we can identify the scattering state from the other

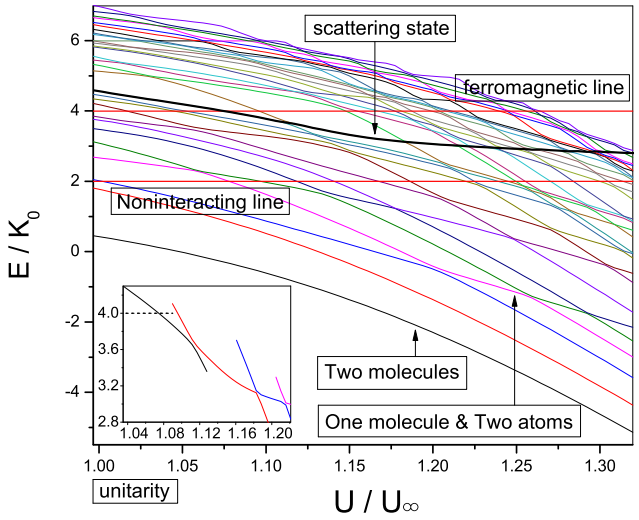

FIG. 4: (Color online) The energy spectrum of the lowest 30 s-states of four fermions with contact interactions on a 3D grid with $n = 10$. The energy levels can be classified into two-molecule states, molecule-atom-atom states and four-atom states. The ferromagnetic transition can be identified as the lowest scattering state (heavy dark line) crossing the horizontal ferromagnetic line around $U/U_\infty \approx 1.07$. The inset shows an enlargement of the lowest scattering state and the associated avoided crossings.

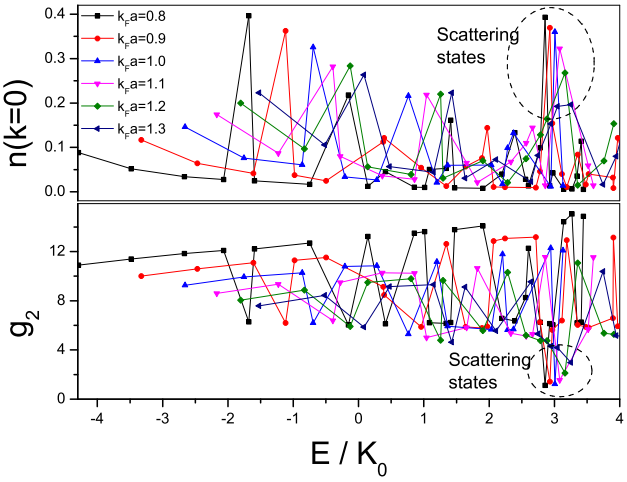

FIG. 5: (Color online) The momentum distribution $n(\mathbf{k} = 0)$ and the pairing parameter g_2 of the lowest 30 s-states of four fermions with contact interactions on a 3D grid with $n = 10$ versus energy. Scattering states have, by definition, $E/K_0 > 2$ and can be identified by the large magnitude of $n(\mathbf{k} = 0)$ and small magnitude of g_2 compared to the other states. The peak structure at the scattering state diminishes as the interaction parameter $k_F a$ increases.

states by the magnitude of g_2: scattering states have a smaller fraction of double occupation $\mathbf{r}_i = \mathbf{r}_j$. Note that the contact C measures the local density of pairs [20]. The momentum distribution $n(\mathbf{k} = 0)$ and the pair parameter g_2 are plotted in Fig (5) as functions of the energy for $k_F a = 0.8 \sim 1.3$. Scattering states are, by definition, in the range $E/K_0 > 2$ and can be identified by the peaks of $n(\mathbf{k} = 0)$ and low values of g_2.

VI. COMPARISON OF THE SLA AND EXACT RESULTS

The ferromagnetic transition in the four-atom system occurs when the scattering state energy equals the non-interacting energy, $4K_0$. For a $n = 10$ grid, the transition occurs at $U/U_\infty \approx 1.07$. Shown in Fig (6) is the energy of the four-particle unpolarized scattering state as a function of the scattering length $k_F a$ on grids with $n = 6, 8, 10, 12$ and their extrapolation to the continuum limit, $n = \infty$. Avoided crossings between levels appear as kinks. The excited scattering state from the solution of the four-particle problem crosses the ferromagnetic line at $k_F a \approx 1.8$, which is in remarkable agreement with the reported experimental value of $k_F a = 1.9 \pm 0.2$ [5].

Also shown is the scattering energy using the SLA; this gives a ferromagnetic transition at $k_F a \approx 1.08 \sim 1.09$ for grid sizes $n = 8, 10, 12$, consistent with previous calculations [3, 4, 7–10]. The earliest Fixed-node diffusion Monte Carlo calculations employed the repulsive Pöschl-Teller potential ($k_F a \approx 0.86$) [8], hard spheres or repulsive soft spheres ($k_F a \approx 0.82$) [9] and included backflow effects ($k_F a \approx 0.96$) [10]. For attractive interactions modeled by spherical square wells or attractive Pöschl-Teller potential, either variational Monte Carlo ($k_F a \approx 0.86$) [9] or fixed-node diffusion Monte Carlo [10] ($k_F a \approx 0.89$) calculates the upper-branch metastable state by imposing a nodal condition in the many-body wave function. The nodal condition ensures that the calculation consist of unbound fermionic atoms and no dimers or other bound molecules, by introducing a Jastrow factor in the form of the scattering solution of the attractive potential corresponding to positive energy. As shown in Sec. III, the nodal structure obtained this way deviates significantly from the true nodes in the upper branch. This explains why all these calculations gave results similar to those from repulsive potentials, and all of them reproduced the predicted behavior of the mean field theory and second order corrections.

The discrepancy between the critical values of $k_F a$ reflects the limitations of perturbation theory in the regime of strong coupling. Compared to repulsive potentials, using Jastow factor with nodes and including backflow effects for attractive potentials improves the result by making nontrivial modifications to the nodal structure, but still gives answers not qualitatively different from the repulsive potential, and fails to reveal the inadequacy of the SLA.

These observations suggest that lower-lying molecular

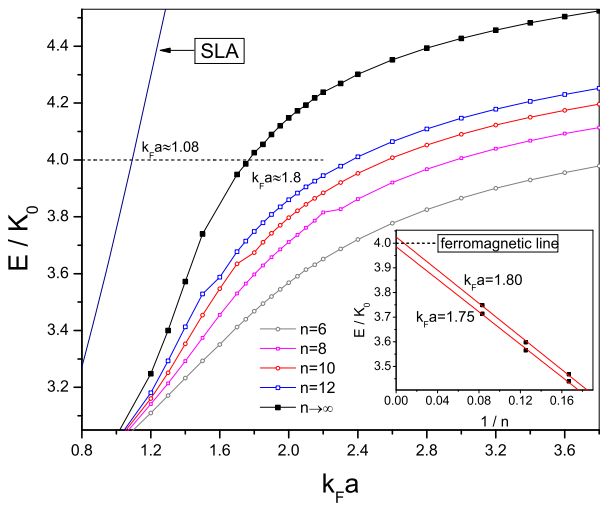

FIG. 6: (Color online) The four particle scattering energy as a function of the scattering length. The energy of the ferromagnetic state is shown as the dashed horizontal line. The extrapolation to continuum is performed based on calculations on grids with $n = 6, 8, 10, 12$, which exhibits the 1^{st}-order linear scaling $1/N$ to high accuracy. The transition to the ferromagnetic phase occurs at $k_F a \approx 1.8$ while the SLA gives the transition at $k_F a \approx 1.08$. The inset shows the scaling with respect to $1/n$ near the transition point $k_F a = 1.75$ and 1.8.

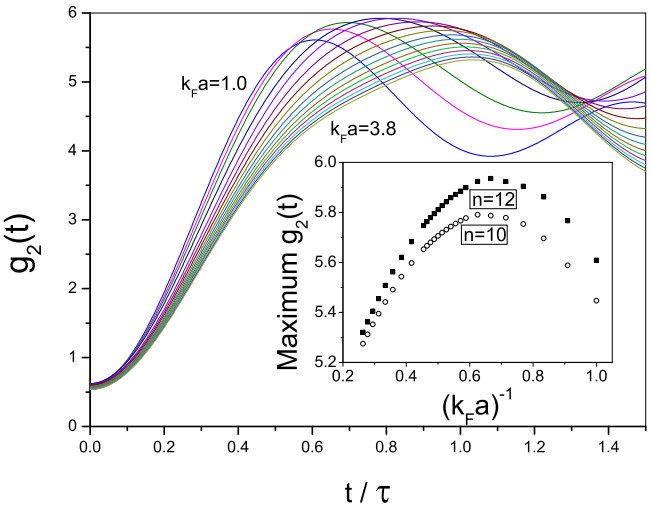

FIG. 7: (Color online) The first oscillation period in the evolution of $g_2(t)$ after a quench from a non-interacting state to an interaction strength $k_F a$, where $\tau = \hbar/\epsilon_F$. The inset shows the nonmonotonic behavior of the maximum value of $g_2(t)$ in the first oscillation period as a function of the final interaction strength $k_F a$. This calculation in done for four particles on a grid with $n = 12$.

states are responsible for delaying the formation of the ferromagnetic phase. However, calculations with more than 4 atoms are needed to determine finite size effects. Such calculations are not feasible with the current method but might be possible with stochastic methods.

VII. DYNAMICS OF FOUR-PARTICLE MODEL

Because of the limited lifetime of the strongly interacting gas, however, the magnetic field ramp in experiment is not adiabatic and can lead to different explanations[21, 22]. A recent work [23] takes into account the effect of atom loss by including a fictitious three-body term in the effective Hamiltonian of the Fermi gas and found that the critical interaction strength required to stabilize the ferromagnetic state increases significantly. A full T-matrix analysis [21] suggests that the pairing instability can prevail over the ferromagntic instability and the experimentally measured atom loss rate can be qualitatively explained in terms of the growth rate of the pairing order parameter after a quench.

Thus, it is an interesting problem to study the dynamics of the pairing instability after a quench using the wave functions obtained in this work. Since the contact C is identified as the integral over space of the expectation value of a local operator that measures the density of pairs [20], we characterize the pairing instability by the count of double occupancy g_2 in Eq (9). To study the dynamics of the pair formation, we choose the initial state to be the unpolarized four-particle ground-state in the noninteracting limit and expanded in the basis of the lowest 16 eigenstates with the final interaction after the quench. The time evolution is then evaluated using the eigenstate expansion $|\psi(t)\rangle = \sum_m c_m e^{-\frac{i}{\hbar}E_m t}|\phi_m\rangle$. The pairing density $g_2(t) = \langle\psi(t)|g_2|\psi(t)\rangle$ is used to characterize the pair formation and the atom loss into molecules. The evolution diagram of $g_2(t)$ is shown in Fig (7). The nonmonotonic dependence of the maximum value of $g_2(t)$ in the first oscillation period on the final scattering length $k_F a$ after the quench is in qualitative agreement with experiment and the full T-matrix theory [21].

VIII. SUMMARY

In summary, we have assessed the accuracy of the scattering length approximation at high density or strong interaction $k_F a \gtrsim 1$. It is demonstrated that if molecular states mix with excitations, non-magnetic states are stabilized. Identification of the upper branch in many-body calculations is discussed. The corresponding nodal structures of the states are examined. The calculated critical interaction strength $k_F a$ for ferromagnetic transition is shown to be underestimated by a factor of two under the scattering length approximation. Although we solved the problem only for 4 particles, this minimal model suffices to show that ignoring the molecular states with the scat-

tering length approximation leads to inaccurate results in the strongly interacting regime. Hence it leads to severe errors in many-body calculations. That we get very good agreement with experimental estimates is encouraging but could be a result of cancellation of errors between the 4 particle system and the thermodynamic limit. We investigated the dynamics of pair formation. Non-monotic behavior of the pairing parameter $\sum_{i<j} \delta_{\mathbf{r}_i,\mathbf{r}_j}$ is observed as a function of the final interaction strength $k_F a$ after a quench.

Acknowledgments—This work has been supported with funds from the DARPA OLE Program and ARO (Grant no. 56693PH), computer time at NCSA. This work was initiated at the Kavli Institute of Theoretical Physics in Beijing and Santa Barbara.

[1] F. Bloch, Z. Phys. **57**, 545 (1929).
[2] F. H. Zong, C. Lin, and D. M. Ceperley, Phys. Rev. E **66**, 036703 (2002).
[3] E. C. Stoner, Philos. Mag. **15**, 1018 (1933).
[4] R. A. Duine and A. H. MacDonald, Phys. Rev. Lett. **95**, 230403 (2005).
[5] Gyu-Boong Jo, *et al.*, Science, **325**, 1521 (2009).
[6] L. J. LeBlanc, *et al.*, Phys. Rev. A **80**, 013607 (2009)
[7] A. Recati and S. Stringari, Phys. Rev. Lett. **106**, 080402 (2011).
[8] G. J. Conduit, A. G. Green and B. D. Simons, Phys. Rev. Lett. **103**, 207201 (2009).
[9] S. Pilati, G. Bertaina, S. Giorgini and M. Troyer, Phys. Rev. Lett. **105**, 030405 (2010).
[10] S. Chang, M. Randeria, and N. Trivedi, PNAS **108**, 51-54 (2011).
[11] Chia-Chen Chang, Shiwei Zhang, and D. M. Ceperley, Phys. Rev. A **82**, 061603(R) (2010).
[12] J. Carlson, *et al.*, Phys. Rev. Lett. **91**, 050041 (2003)
[13] A finite-difference expression for the Laplacian operator is $-\nabla^2\psi_i = \Delta^{-2}\sum_{j=-n/2}^{n/2} c_j\psi_{i+j}$. The coefficients c_j are obtained through the Fourier expansion of the eigenvalues of the Laplacian $k^2 = c_0 + 2\sum_{j=1}^{n/2} c_j \cos(kj)$ and are given in Table I of Ref.[14]. This expression also gives the single particle dispersion relation ϵ_k in one dimension.
[14] J. R. Chelikowsky, *et al.*, Phys. Rev. B **50**, 11355 (1994).
[15] Y. Castin, J. Phys. IV 116, **89** (2004).
[16] K. A. Bruekner, Phys. Rev. **89**, 834 (1953).
[17] L. D. Landau and E. M. Lifshitz, *Quantum Mechanics, non-relativistic theory* (Butterworth-Heinemann, 1981).
[18] D. C. Mattis, Rev. Mod. Phys. **58**, 361-379 (1986).
[19] S. Tan, Ann. Phys. (N.Y.) 323, 2971 (2008);
[20] E. Braaten and L. Platter, Phys. Rev. Lett. **100**, 204301 (2008).
[21] D. Pekker, *et al.*, Phys. Rev. Lett. **106**, 050402 (2011).
[22] H. Zhai, Phys. Rev. A **80**, 051605 (2009).
[23] G. J. Conduit and E. Altman, Phys. Rev. A **83**, 043618 (2011).
[24] G. B. Partridge, *et al.*, Phys. Rev. Lett. **95**, 020404 (2005).